19 July 2001

PHYSICS LETTERS B

Physics Letters B 512 (2001) 268–276

www.elsevier.com/locate/npe

Identification of excited structures in proton unbound nuclei ^{173,175,177}Au: shape co-existence and intruder bands

F.G. Kondev [a,b], M.P. Carpenter [a], R.V.F. Janssens [a], K. Abu Saleem [a,c], I. Ahmad [a], H. Amro [a,d], J.A. Cizewski [e], M. Danchev [f], C.N. Davids [a], D.J. Hartley [f], A. Heinz [a], T.L. Khoo [a], T. Lauritsen [a], C.J. Lister [a], W.C. Ma [d], G.L. Poli [a], J. Ressler [a,g], W. Reviol [f,h], L.L. Riedinger [f], D. Seweryniak [a,g], M.B. Smith [e], I. Wiedenhöver [a,1]

[a] *Physics Division, Argonne National Laboratory, Argonne, IL 60439, USA*
[b] *Technology Development Division, Argonne National Laboratory, Argonne, IL 60439, USA*
[c] *Department of Physics, Illinois Institute of Technology, Chicago, IL 60616, USA*
[d] *Department of Physics, Mississippi State University, Starkville, MS 39762, USA*
[e] *Department of Physics and Astronomy, Rutgers University, N. Brunswick, NJ 08903, USA*
[f] *Department of Physics and Astronomy, University of Tennessee, Knoxville, TN 37996, USA*
[g] *Department of Chemistry, University of Maryland, College Park, MD 20742, USA*
[h] *Department of Chemistry, Washington University, St. Louis, MO 63130, USA*

Received 2 March 2001; received in revised form 10 April 2001; accepted 11 May 2001
Editor: V. Metag

Abstract

Excited states in the proton-unbound ^{173,175,177}Au nuclei were identified for the first time. Level structures associated with three different shapes were observed in ^{175}Au. While the yrast lines of ^{175}Au and ^{177}Au consist of a prolate band built upon the intruder $1/2^+[660]$ ($i_{13/2}$) proton orbital, no sign of collectivity was observed in the lighter ^{173}Au isotope. Implications for the deformation associated with these structures are discussed with a focus on shape co-existence in the vicinity of the proton-drip line. © 2001 Published by Elsevier Science B.V.

PACS: 27.70.+q; 23.20.Lv; 23.60.+e; 21.10.Tg

Even–even neutron-deficient nuclei near the $Z = 82$ shell closure are known to exhibit coexistence between an oblate or nearly spherical ground state and a prolate shape located only a few hundred keV higher in excitation energy [1,2]. Recently, it has been shown that the prolate minimum increases in energy with respect to the ground state as the neutron number decreases below mid-shell ($N \sim 104$) [3–8]. At present, the role of individual proton and neutron orbitals in driving the nuclear shape has not been fully delineated. The present Letter addresses the role of protons by providing detailed information on the level structures of the most neutron-deficient Au nuclei investigated thus far.

The study of these nuclei is of importance not only in the context of shape coexistence, but also in relation to the accurate description of proton emitters. It

E-mail address: kondev@anl.gov (F.G. Kondev).

[1] Present address: National Superconducting Cyclotron Laboratory, Michigan State University, East Lansing, MI 48824, USA.

0370-2693/01/$ – see front matter © 2001 Published by Elsevier Science B.V.
PII: S0370-2693(01)00714-6

has been shown that proton decay rates, which depend on the tunneling probability through the Coulomb and centrifugal barriers, are sensitive not only to the quantum numbers and the intrinsic configurations of the parent and daughter nuclei, but also to other important structural effects, most notably deformation [9,10]. In the region near the $Z = 82$ shell closure, effects of deformation on the properties of proton emitters should be expected because of the shape coexistence mentioned above and the ensuing interaction between configurations associated with the different shapes. However, the experimental situation is unclear because the degree to which this coexistence persists in drip line nuclei is poorly known. Proton emitters in ^{171}Au [11] and ^{177}Tl [12] were interpreted as resulting from the coupling of the $\pi h_{11/2}$ orbital to the *near-spherical* ground state of the even–even core. The proton decay rate in ^{185}Bi [13] was also reproduced satisfactorily with a configuration consisting of a $s_{1/2}$ proton coupled to the $(\pi h_{9/2})^2$ core, although the influence of the *oblate* shape associated with this intruder configuration was not explicitly considered in the calculations.

The limited knowledge about shape evolution near the proton-drip line in this mass region is partly due to experimental difficulties in the production of states of high spin and excitation energy in the nuclei of interest by using conventional heavy-ion fusion reactions because of severe competition from fission. Furthermore, the small evaporation-residue cross section is also fragmented over many channels, thus requiring sensitive detection techniques to select a specific nucleus. One such technique is recoil decay tagging (RDT) [14]. It correlates the prompt γ-rays emitted from a recoiling nucleus at the target position with its subsequent characteristic alpha (or proton) decay. Further suppression of fission and charged particle emission can be achieved by taking advantage of fusion reactions between symmetric nuclei, which often have large, negative Q-values at energies near the barrier [15].

In this Letter, we report on the observation of excited structures in the ^{173}Au ($N = 94$), ^{175}Au ($N = 96$) and ^{177}Au ($N = 98$) isotopes. These nuclei provide the opportunity to elucidate the shape driving properties of proton excitations based on the important $h_{9/2}$, $f_{7/2}$ and $i_{13/2}$ *proton* orbitals in a region where they have not been investigated much before, e.g., below mid-shell. In addition, the role of the low-Ω $i_{13/2}$ neutrons can also be examined. The impact of the latter on the formation of different minima has been largely neglected in this mass region. All three Au isotopes are energetically unbound to the emission of protons [9], but their decay via α emission is favored by the associated Q values and barrier heights. The yrast structures of ^{175}Au and ^{177}Au are found to be the result of the coupling of an intruder $i_{13/2}$ proton to the prolate deformed Pt and Hg cores identified previously [5–8]. Remarkably, no sign of collectivity is observed in the lightest isotope, ^{173}Au. Theoretical calculations of occupation probabilities and single-particle quadrupole moments show a correlation between the magnitude of the deformation of the intruder bands and the population of low-Ω $h_{9/2}$ proton and $i_{13/2}$ neutron orbitals.

Excited states in ^{173}Au, ^{175}Au and ^{177}Au were populated via the $p2n$ channels in fusion reactions of ^{84}Sr ions with ^{92}Mo (at 390 and 395 MeV beam energy), ^{94}Mo (380 and 385 MeV) and ^{96}Mo (380 MeV) targets. The beam was delivered by the ATLAS superconducting linear accelerator at Argonne National Laboratory. The isotopically enriched ($> 90\%$), self-supporting targets were about 700 μg/cm^2 thick. Prompt γ-rays were detected with the Gammasphere array [16] consisting, for these experiments, of 101 large volume escape-suppressed Ge detectors. The evaporation residues were transported through the Fragment Mass Analyzer (FMA) [17] and were dispersed according to their mass-to-charge (m/q) ratio. A position-sensitive parallel grid avalanche counter (PGAC), located at the FMA focal plane, provided the m/q information and the time of arrival of the recoils. The latter nuclei were subsequently implanted into a 40×40 (40×40 mm, ~ 60 μm thick), double-sided silicon strip detector (DSSD) located 40 cm behind the PGAC. Each event in the DSSD was time stamped and identified as either an implanted recoil or a charged-particle decay, depending on the correlation with a signal from the PGAC. The background introduced by scattered projectiles, which have much higher velocities than the evaporation residues, was removed in the off-line analysis by placing coincidence gates on the evaporation-residue events in the two-dimensional histogram of the time-of-flight between PGAC and DSSD versus the implantation energy. In addition, an array consisting of four Gammasphere-type Ge de-

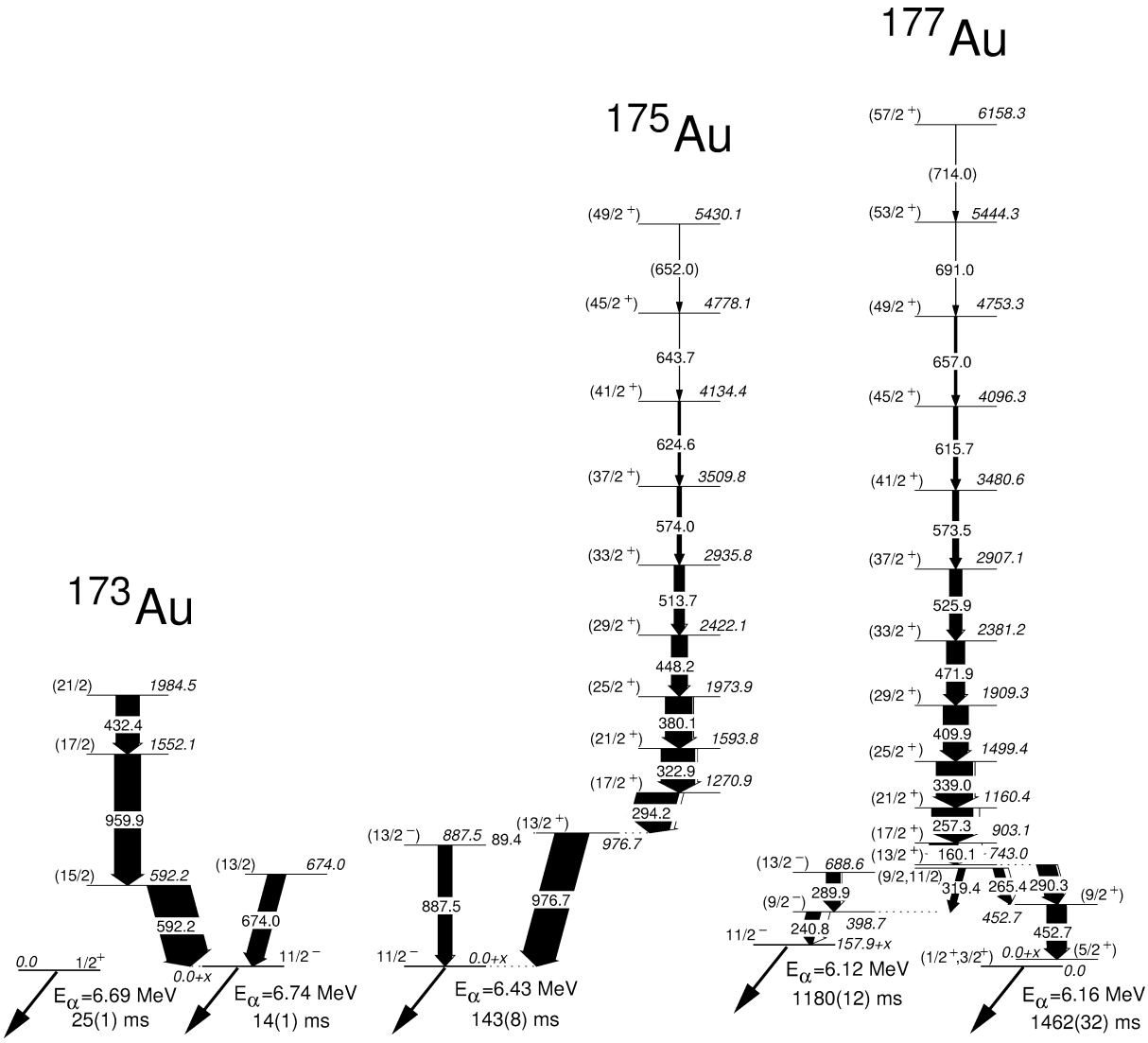

Fig. 1. Partial level scheme for the yrast cascades in ^{173}Au, ^{175}Au and ^{177}Au. The width of the arrows is proportional to the intensity of the transitions. The α-decaying states are indicated with the corresponding energies and half-lives.

tectors and a single low-energy photon spectrometer (LEPS) surrounded the DSSD. Time-correlated, α–γ coincidences were measured and used to elucidate the α-decay fine structure to excited levels in daughter and grand-daughter nuclei and, hence, to provide unambiguous spin, parity and configuration assignments to the α-decaying states. Specific details regarding the experiments and the data reduction can be found in Ref. [18].

Partial level schemes showing the yrast structures of ^{173}Au, ^{175}Au and ^{177}Au are presented in Fig. 1. A common feature in all three cases is the presence of an α-decaying, high-spin isomer. The measured α-decay energies and half-lives were found to be in agreement with the most recently published values [12,19], but in general the present results are of greater accuracy. Furthermore, the presence of two α-emitting states in ^{177}Au was firmly established, con-

trary to the conclusion drawn in Ref. [20]. Based on the deduced α-decay reduced widths, the observed α–γ correlations and the available experimental information about the daughter and grand-daughter nuclei [21–24], the high-spin isomers are assigned $I^\pi = 11/2^-$ and the $11/2^-[505]$ ($h_{11/2}$) Nilsson configuration. The shape associated with this orbital changes gradually as the neutron number decreases from triaxial in ^{185}Au [25] ($N = 106$) to nearly spherical in ^{171}Au [11] ($N = 92$). A low spin isomer has also been observed in ^{173}Au and ^{177}Au, but not in ^{175}Au. Poli et al. [12] proposed a $1/2^+[400]$ ($s_{1/2}$) configuration to this state in ^{173}Au. Given the distribution of single-particle states near the proton Fermi surface and the limited decay information available on the daughter ^{173}Ir [21] and parent ^{181}Tl [26] nuclei, a tentative ($1/2^+$, $3/2^+$) assignment is proposed for the isomer in ^{177}Au. The most likely configuration is either $1/2^+[411]$ ($d_{3/2}$) at oblate deformation, or $3/2^+[402]$ ($d_{3/2}$) at prolate deformation, albeit some $s_{1/2}$ admixture should also be expected. It is worth pointing out that the structure of the low-lying states in ^{173,175,177}Au differs significantly from that seen in the heavier ^{179,181,183,185}Au nuclei where ground states are assigned $I^\pi = 5/2^-$ and are understood as members of the intruder $\pi h_{9/2}$ band [25,27,28]. This feature is indicative of a shape change which occurs in this isotopic chain in a manner similar to that observed in the even–even Pt core nuclei (see, for example, Refs. [3–6] and references therein).

Sample γ-ray spectra showing transitions depopulating states in ^{173}Au, ^{175}Au and ^{177}Au are given in Fig. 2. The assignment of γ-rays to a specific isotope is based on correlations with the characteristic α-decay line and with the gold X-rays. The placement of transitions and levels is determined from the γ-ray coincidence relationships. Their ordering follows from the relative intensities within a given cascade. Since γ-ray angular distributions were found to be nearly isotropic within statistical uncertainties, presumably as a result of de-orientation as the ions recoil into vacuum [29], it was not possible to obtain useful information on transition multipolarities. However, γ-ray intensity balances were used to extract total electron-conversion coefficients, α_T, in order to distinguish between E1, M1 or E2 character for transitions with energies below about 250 keV for which the conversion coefficients are significantly different. Although most assignments remain tentative, the proposed spins and parities are consistent with the analysis of a range of additional information, including spectroscopic data on the daughter and grand-daughter nuclei, and systematics in heavier Au [25,27,28,30] and Tl [31–33] isotopes.

At high spin, the yrast line of ^{177}Au comprises a well-deformed prolate band. While intensity considerations established an E2 multipolarity for the 160.1 keV transition ($\alpha_T(\text{exp}) = 0.70(7)$; $\alpha_T(\text{E1}) = 0.13$, $\alpha_T(\text{E2}) = 0.84$, $\alpha_T(\text{M1}) = 1.97$ [34]), other in-band transitions are assumed to be of E2 character. Below the $(13/2^+)$ level, the intensity flux splits into two branches, one proceeds via the 319.4, 289.9 and 240.8 keV transitions through the $(9/2^-)$ member of the $\pi h_{9/2}$ band and the $11/2^-$ isomer, while the other reaches the ($1/2^+$, $3/2^+$) ground state via the 265.4, 290.3 and 452.7 keV γ-rays. The lack of intensity balance at the 398.7 keV level indicates that a short lifetime ($T_{1/2} \leqslant 15$ ns) may be present. Although the experiment is not sensitive to direct measurements of the half-life, it is worth pointing out that a value of about 17 ns would be expected for this state, based on the strength of $8.4(7) \times 10^{-5}$ (μ_N^2) measured for an analogous $11/2^- \to 9/2^-$ M1 transition in ^{185}Au [35]. The yrast line of ^{175}Au is also formed by a collective band, similar to that seen in ^{177}Au, but its decay proceeds entirely through the $11/2^-$ isomer. The E1 character of the 89.4 keV transition follows from intensity balance considerations, and other in-band transitions are assumed to be stretched quadrupoles. In contrast to ^{175}Au and ^{177}Au, no sign of collectivity is observed in ^{173}Au. The 592.2, 959.9 and 432.4 keV transitions are observed to be in coincidence with each other and their ordering within a cascade follows from the measured relative intensities. The 674.0 keV γ-ray was not in coincidence with the above transitions and is placed as a direct feeding of the $11/2^-$ isomer. Two additional γ-rays, with energies of 748.0 and 803.0 keV, are seen in the spectrum of Fig. 2(a). These were not placed in the level scheme because of their weak intensities. Additional band structures were observed in ^{175}Au and ^{177}Au. The complete level schemes are beyond the scope of the present work and will be discussed elsewhere [36].

Positive parity yrast bands are known in the heavier odd-mass Au [25,27,28,30] and Tl [31–33] nuclei.

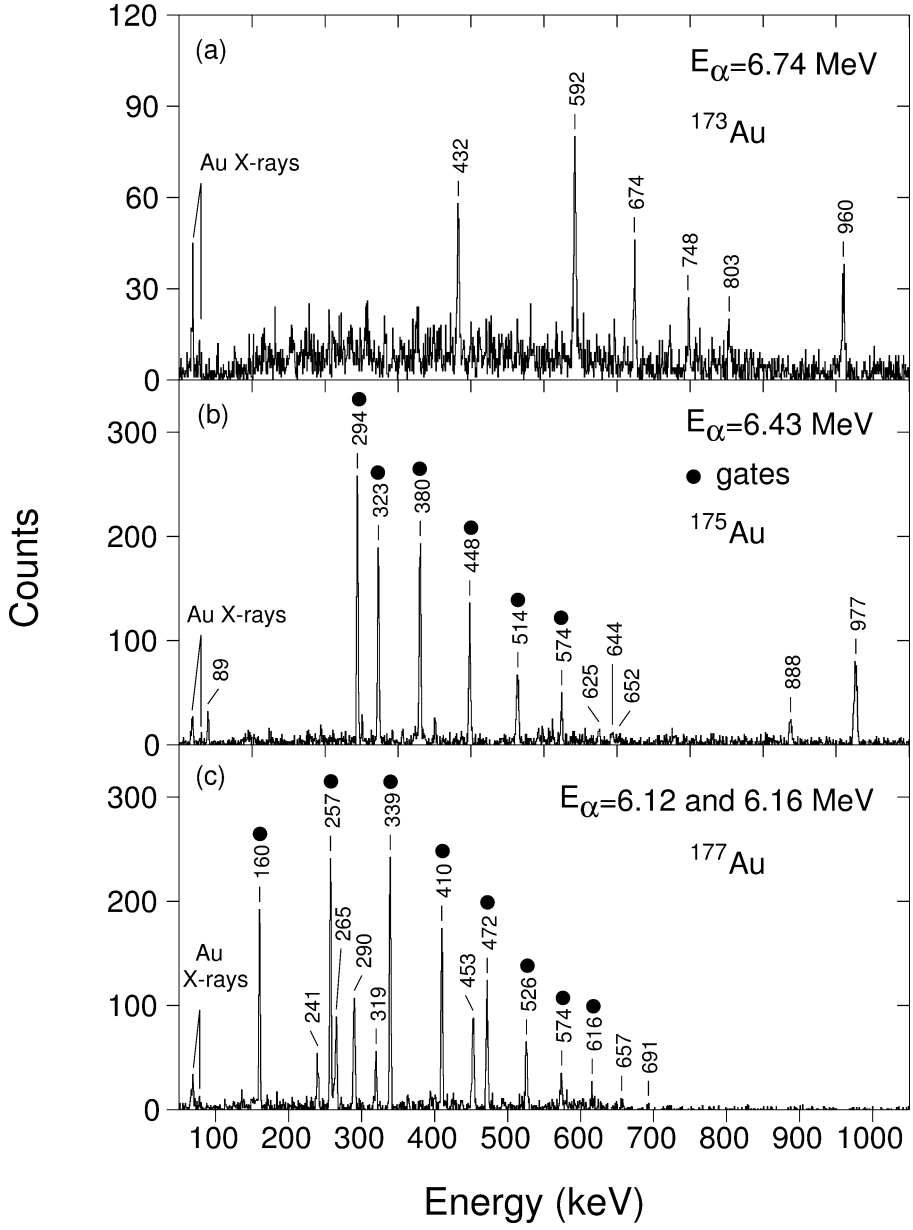

Fig. 2. (a) Spectrum of γ-rays correlated with the ^{173}Au α-decay line of $E_\alpha = 6.74$ MeV. Summed, background-subtracted γ-ray coincidence spectra from the α–γ–γ matrix produced by gating on the $E_\alpha = 6.43$ MeV (^{175}Au) line (b) and on the $E_\alpha = 6.12$ and 6.16 MeV (^{177}Au) lines (c). The transitions used as gates are indicated with filled circles.

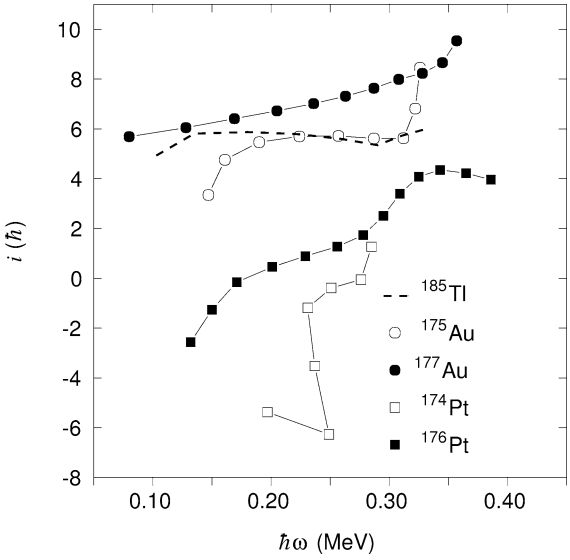

Fig. 3. Aligned angular momenta for the yrast bands in ^{175}Au and ^{177}Au, and their even–even Pt core nuclei. The dashed line represents the aligned angular momentum seen in ^{185}Tl [31], a mid-shell nucleus representative of all deformed Tl nuclei. The same reference parameters, $\Im_0 = 27.5\ \mathrm{MeV}^{-1}\,\hbar^2$ and $\Im_1 = 190.0\ \mathrm{MeV}^{-3}\,\hbar^4$, have been used for all bands.

They have been associated with a prolate shape and assigned to the intruder $1/2^+[660]$ ($i_{13/2}$) proton configuration. A characteristic feature of these structures is strong Coriolis mixing which leads to a large alignment ($i \approx 6\hbar$) and a sizable signature splitting, with only the favored signature being observed. The newly established bands in ^{175}Au and ^{177}Au are consistent with such an interpretation.

Experimental alignments for the positive parity sequences in ^{175}Au and ^{177}Au are compared with those of their even–even platinum [5,6] cores and neighboring odd-Z Tl [31–33] isotopes in Fig. 3. The observed values of $i \sim 6\hbar$ for the bands in ^{175,177}Au are consistent with expectations for a rotationally-aligned $i_{13/2}$ proton, and support the $1/2^+[660]$ configuration assignment. At the lowest frequencies, the Pt nuclei show an increase in alignment caused by a change from an oblate to a more deformed prolate shape [5,6]. The yrast sequence in ^{175}Au exhibits a related behavior, thus suggesting that a similar shape change may have occurred. This is also evident from the spectrum shown in Fig. 2(b), where the 294.2 keV transition does not follow the regular collective pattern established by the higher-energy transitions and, therefore, cannot be interpreted as a member of the rotational cascade. In addition, a variable moment of inertia (VMI) fit (see below) applied to the levels between $(17/2^+)$ and $(49/2^+)$, predicts an energy of about 199 keV for the $17/2^+ \to 13/2^+$ in-band transition. In this mass region an oblate to prolate shape change is a well established phenomenon. It occurs along the positive-parity, yrast structures in the heavier odd-Z ^{185,187,189}Tl isotopes [31,33]. In fact, while the $1/2^+[660]$ ($i_{13/2}$) *prolate* band has been observed to be yrast at high spin in these nuclei, the lowest $13/2^+$ state has been assigned to the $13/2^+[606]$ ($i_{13/2}$) *oblate* configuration. Taking into account the striking similarities between the present observations for ^{175}Au and these positive-parity Tl sequences, the same $13/2^+[606]$ *oblate* configuration is proposed for the $(13/2^+)$ state at 976.7 keV. In terms of shape coexistence, it is worth noting that structures associated with *three* different shapes compete for yrast status in ^{175}Au. A near-spherical ground state ($I^\pi = 11/2^-$) is followed by the $(13/2^+)$ oblate level while the prolate band dominates at higher spins. The energy separation between the observed states can be associated with the energy difference between these minima, albeit the excitation energy of the prolate well is more subtle since the $i_{13/2}$ prolate band is not observed down to its bandhead, presumably due to effects associated with deformation and Coriolis mixing.

Similar to the approach outlined in Ref. [31], a so-called VMI fit was carried out for the $i_{13/2}$ bands in ^{175,177}Au, as well as for those of the heavier odd-mass gold isotopes [25,27,28,30]. Empirical values of the deformation were subsequently deduced using $\beta_2 \approx 91.7 Q_0/ZA^{2/3}$ [37], with a quadrupole moment estimated as $Q_0 \approx 39.4\sqrt{\Im_0}$ [38], where $\Im_0$ is the moment of inertia. The results are presented in the upper part of Fig. 4, together with predictions given by total Routhian surface (TRS) calculations based on a Woods–Saxon potential [39]. It is apparent that the deformation of the $i_{13/2}$ band in ^{177}Au is larger than that in ^{175}Au. Such a difference would account for the larger alignment observed for the former band (see Fig. 3). By extrapolating the trend seen in Fig. 4(a) towards lower neutron number, one would expect an even smaller deformation for the $i_{13/2}$ band in ^{173}Au, a structure which has not been observed in the current work. It is also interesting to note that while the TRS

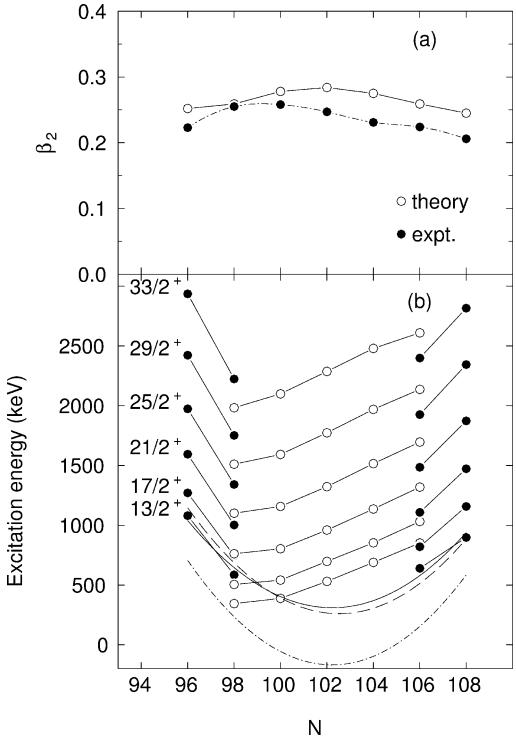

Fig. 4. (a) Equilibrium deformations for the $1/2^+[660]$ ($i_{13/2}$) configuration over a range of gold isotopes. The filled symbols correspond to the values deduced from the VMI fit, while the open symbols are predictions from TRS calculations (see text for details). (b) Energy systematics for the prolate $1/2^+[660]$ ($i_{13/2}$) band in the odd-mass Au isotopes relative to the $11/2^-$ ($h_{11/2}$) intrinsic state (filled symbols) and the $9/2^-$ member of the $h_{9/2}$ band (open symbols). The results for the heavier Au nuclei are taken from Refs. [25,27,28,30]. The position of the $13/2^+$ level in ^{175}Au has been deduced from the VMI fit, as discussed in the text. The parabolic fit for the $\pi i_{13/2}$–$\pi h_{11/2}$ energy differences in the Au isotopes are shown by the solid line. The dashed and the dot-dashed lines represent fits to the prolate–oblate energy differences in the neighboring even–even Hg and Pt isotopes, respectively.

predictions placed the maximum in deformation near mid-shell, the extracted empirical values maximize at lower neutron number ($N \sim 98$–100). The reason for such a difference is at present not fully understood. It is interesting to speculate that this may be due in part to changes in the shell structure associated with weak binding. On the other hand, it is worth pointing out that, at $N = 98$, the neutron Fermi level resides at the boundary of a deformed ($\beta_2 \sim 0.25$) sub-shell gap and that this results in an increased shell-stability for specific prolate configurations.

In order to gain further insight into the differences in deformation noted above, calculations of the single-particle quadrupole moments and of the occupation probabilities of various orbitals were carried out using a Woods–Saxon potential with the Lipkin–Nogami treatment of pairing in a way similar to that of Ref. [31]. Fig. 5 shows the contribution of specific orbitals to the deformation of the $i_{13/2}$ bands in ^{173,175,177}Au. The importance of the $1/2^-[541]$ ($h_{9/2}$) orbital in the formation of the prolate minimum has been noted before (e.g., Refs. [2,31]) and is also evident in Fig. 5(a). The correlation between the change in deformation with neutron number and the occupation of the low-Ω $i_{13/2}$ *neutrons* is also apparent. Hence, one may conclude that the decrease in deformation of the $i_{13/2}$ bands in the odd-mass Au nuclei with neutron number is, at least partially, due to the step-wise decrease in the occupations of the low-Ω $i_{13/2}$ neutron orbitals, as well as to the $h_{9/2}$ proton orbital.

Fig. 4(b) compares the excitation energies of the $1/2^+[660]$ ($i_{13/2}$) band members relative to the $11/2^-$ ($h_{11/2}$) and the $9/2^-$ ($h_{9/2}$) states in several odd-mass gold isotopes. The parabolic fit to the $\pi i_{13/2}$ (prolate)–$\pi h_{11/2}$ (near-spherical/weakly-deformed) energy differences shows a minimum near mid-shell and resembles closely the prolate–oblate energy differences observed in neighboring even–even Pt and Hg isotopes. Another feature shown in Fig. 4(b) is that the $\pi i_{13/2}$ (prolate)–$\pi h_{9/2}$ (prolate) energy difference continues to decrease below mid-shell. Such a behavior should not be a surprise, given the deformation differences between these two orbitals, as recently discussed by Lane et al. [31]. It should be also noted that the effects of Coriolis coupling and triaxiality were not taken explicitly into account in the systematics shown in Fig. 4(b), although their role may be significant as the deformation reaches smaller values.

To summarize, excited structures in the neutron deficient ^{173}Au, ^{175}Au and ^{177}Au nuclei were observed for the first time using the Gammasphere array and the recoil-decay tagging method. These data provide a link between heavier deformed Au nuclei ($N > 100$) and the spherical proton-emitter ^{171}Au. In this context, ^{175}Au (with levels associated with three different shapes) presents itself as a transitional nucleus. Theoretical calculations of intruder orbital occupation probabilities and single-particle quadrupole moments

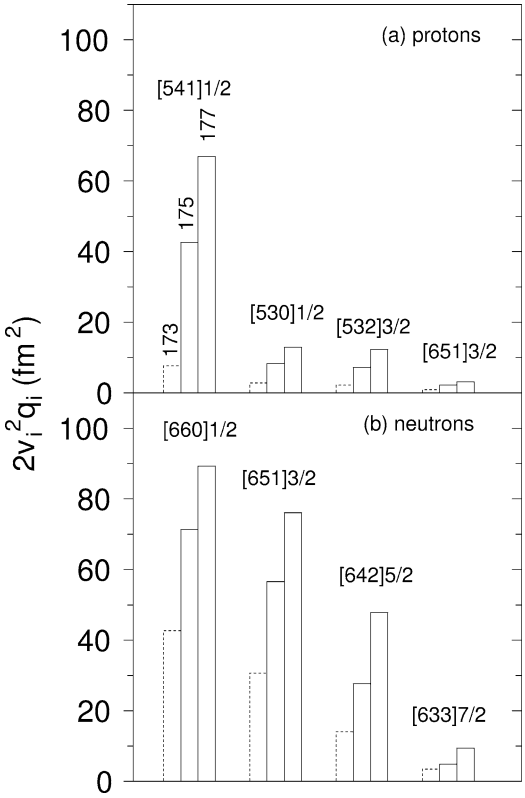

Fig. 5. Predicted contributions of the main intruder proton (a) and neutron (b) orbitals to the quadrupole deformation of ^{173}Au (left bin), ^{175}Au (middle) and ^{177}Au (right) nuclei. The single-particle quadrupole moments (q_i) and energies were calculated using the Woods–Saxon potential with "universal" parameterization [40] and deformations $\beta_2 = 0.170$ (^{173}Au), $\beta_2 = 0.223$ (^{175}Au) and $\beta_2 = 0.255$ (^{177}Au) ($\beta_4 = -0.005$ in all cases). The β_2 value for ^{173}Au does not come from experimental data since the rotational band of interest has not been observed. Instead, this deformation value has been deduced by extrapolating the experimental data presented in Fig. 4(a). The corresponding occupation probabilities are shown as dashed lines in order to remind the reader of the additional uncertainties associated with this extrapolation. The occupation probabilities, v_i, were calculated using the Lipkin–Nogami treatment of pairing with $G_\nu = 18.0/A$ (MeV) and $G_\pi = 20.8/A$ (MeV). In the calculation the proton $1/2^+[660]$ ($i_{13/2}$) orbital was occupied (blocked), thus having an occupational probability of unity.

show a correlation between the magnitude of the deformation and the pairwise occupation of the $\pi h_{9/2}$ and $\nu i_{13/2}$ orbitals. The observation of deformed, prolate bands in ^{175}Au and ^{177}Au provides evidence that *blocking* of the $1/2^+[660]$ ($i_{13/2}$) orbitals does not preclude the development of the prolate shape. This would imply that more complicated particle–hole excitations are involved in the configuration of the prolate structures in the neutron deficient Au nuclei.

Acknowledgements

The authors express their gratitude to the staff of the ATLAS accelerator for the quality of the beam and to the members of the Physics Division Support Group for their assistance in the preparation of the experiment. FGK gratefully acknowledges discussions with G.D. Dracoulis and G.J. Lane on various aspects of this work. Discussions with G.D. Sprouse are also acknowledged. This work is supported by the U.S. Department of Energy, Nuclear Physics Division, under Contracts No. W-31-109-ENG-38 and DE-FG02-96ER40983.

References

[1] J.L. Wood, K. Heyde, W. Nazarewicz, M. Huyse, P. Van Duppen, Phys. Rep. 251 (1992) 101, and references therein; J.H. Hamilton, Prog. Part. Nucl. Phys. 28 (1992) 87, and references therein.
[2] K. Heyde, P. Van Isacker, M. Waroquier, J.L. Wood, R.A. Meyer, Phys. Rep. 102 (1983) 293.
[3] B. Cederwall et al., Phys. Lett. B 443 (1998) 69.
[4] G.D. Dracoulis, Phys. Rev. C 49 (1994) 3324.
[5] G.D. Dracoulis, B. Fabricius, A.E. Stuchbery, A.O. Macciavelli, W. Korten, F. Azaiez, E. Rubel, M.A. Deleplanque, R.M. Diamond, F.S. Stephens, Phys. Rev. C 44 (1991) R1246.
[6] G.D. Dracoulis, A.E. Stuchbery, A.P. Byrne, A.R. Poletti, J. Gerl, R.A. Bark, J. Phys. G 12 (1986) L97.
[7] M.P. Carpenter et al., Phys. Rev. Lett. 78 (1997) 3650.
[8] M. Muikku et al., Phys. Rev. C 58 (1998) R3033.
[9] P.J. Woods, C.N. Davids, Annu. Rev. Nucl. Part. Sci. 47 (1997) 541.
[10] C.N. Davids et al., Phys. Rev. Lett. 80 (1998) 1849.
[11] C.N. Davids et al., Phys. Rev. C 55 (1997) 2255.
[12] G.L. Poli et al., Phys. Rev. C 59 (1999) R2979.
[13] C.N. Davids et al., Phys. Rev. Lett. 76 (1996) 592.
[14] E.S. Paul et al., Phys. Rev. C 51 (1995) 71; R.S. Simon et al., Z. Phys. A 325 (1986) 197.
[15] F.G. Kondev et al., Nucl. Phys. A 682 (2001) 187c.
[16] I.Y. Lee, Nucl. Phys. A 520 (1990) 641c.
[17] C.N. Davids, B.B. Back, K. Bindra, D.J. Henderson, W. Kutschera, T. Lauritsen, Y. Nagame, P. Sugathan, A.V. Ramayya, W.B. Walters, Nucl. Instrum. Methods Phys. Res. B 70 (1992) 358.
[18] F.G. Kondev et al., Phys. Rev. C 61 (2000) 044323.

[19] R.D. Page, P.J. Woods, R.A. Cunningham, T. Davinson, N.J. Davis, A.N. James, K. Livingston, P.J. Sellin, A.C. Shotter, Phys. Rev. C 53 (1996) 660.
[20] C. Cabot, C. Deprun, H. Gauvin, B. Lagarge, Y. Le Beyec, M. Lefort, Nucl. Phys. A 241 (1975) 341.
[21] W.-D. Schmidt-Ott, H. Salewski, F. Meissner, U. Bosch-Wicke, P. Koschel, V. Kunze, R. Michaelsen, Nucl. Phys. A 545 (1992) 646.
[22] M.P. Carpenter et al., to be published.
[23] R.A. Bark et al., Nucl. Phys. A 657 (1999) 113.
[24] S. Juutinen et al., Nucl. Phys. A 526 (1991) 346.
[25] A.J. Larabee, M.P. Carpenter, L.L. Riedinger, L.H. Courtney, J.C. Waddington, V.P. Janzen, W. Nazarewicz, J.-Y. Zhang, R. Bengtsson, G.A. Leander, Phys. Lett. B 169 (1986) 21.
[26] K.S. Toth et al., Phys. Rev. C 58 (1998) 1310.
[27] W.F. Mueller et al., Phys. Rev. C 59 (1999) 2009.
[28] W.F. Mueller et al., to be published.
[29] G.D. Sprouse, in: J. Christiansens (Ed.), Hyperfine Interactions of Radioactive Nuclei, Springer-Verlag, Berlin, 1983, p. 15.
[30] A. Korichi, N. Perrin, C. Bourgeois, D. Hojman, D.G. Popescu, H. Sergolle, F. Hannachi, M.G. Porquet, Z. Phys. A 343 (1992) 15.
[31] G.J. Lane, G.D. Dracoulis, A.P. Byrne, P.M. Walker, A.M. Baxter, J.A. Sheikh, W. Nazarewicz, Nucl. Phys. A 586 (1995) 316;
G.J. Lane, G.D. Dracoulis, A.P. Byrne, P.M. Walker, A.M. Baxter, R.G. Henry, D. Nisius, C.N. Davids, T. Lauritsen, H. Penttilä, D.J. Henderson, J.A. Sheikh, W. Nazarewicz, Phys. Lett. B 324 (1994) 14.
[32] W. Reviol et al., Phys. Rev. C 61 (2000) 044310.
[33] M.-G. Porquet et al., Phys. Rev. C 44 (1991) 2445.
[34] R.S. Hager, E.C. Seltzer, Nucl. Data Sheets A 4 (1968) 1.
[35] R.A. Braga, B.E. Gnade, R.W. Fink, H.K. Carter, Nucl. Phys. A 410 (1983) 441.
[36] F.G. Kondev et al., unpublished.
[37] K.E.G. Löbner, M. Vetter, V. Hönig, Nucl. Data Tables A 7 (1970) 495.
[38] M.A.J. Mariscotti, G. Scharff-Goldhaber, B. Buck, Phys. Rev. 178 (1969) 1864.
[39] R. Wyss, W. Satula, W. Nazarewicz, A. Johnson, Nucl. Phys. A 511 (1990) 324.
[40] S. Cwiok, J. Dudek, W. Nazarewicz, J. Skalski, T. Werner, Comput. Phys. Commun. 46 (1987) 379.